The Aharonov-Bohm effect in a mesoscopic ring of diluted magnetic alloy

1992 J. Phys.: Condens. Matter 4 3943

(http://iopscience.iop.org/0953-8984/4/15/009)

J. Phys.: Condens. Matter 4 (1992) 3943–3954. Printed in the UK

The Aharonov–Bohm effect in a mesoscopic ring of diluted magnetic alloy

V I Fal'ko

Max-Planck-Institut für Festkörperforschung, Hochfeld-Magnetlabor, 25 Avenue des Martyrs, Grenoble, France and Theory Department, Institute of Solid State Physics, 142432 Chernogolovka, Moscow District, Russia

Received 6 February 1991, in final form 19 December 1991

Abstract. The spin dynamics of magnetic impurities is shown to play a crucial role in mesoscopic effects. It follows from this analysis that the quantum magnetoconductance oscillations in a mesoscopic ring of a diluted magnetic alloy are gradually suppressed in the paramagnetic regime, whereas a strong magnetic field forbids spin-flip processes and restores the mesoscopic Aharonov–Bohm oscillations with an amplitude limited by the efficiency of electron escape to the bulk. This effect is examined analytically using a model of a quasi one-dimensional ring joined to the electrodes by tunnelling contacts or short leads.

1. Introduction

The quantum interference of electron waves in a small metallic ring is the origin of its transport properties' sensitivity to the enclosed flux ϕ of a magnetic field [1]. An additional phase $\varphi = 2\pi\phi/\phi_0$, due to the electron moving along different paths enclosing the magnetic flux ϕ, raises the $\phi_0 = hc/e$ periodic dependence of all the kinetic coefficients of a circlet prepared from one-dimensional (1D) wires [1, 2] (the Aharonov–Bohm effect). This statement is based on general quantum mechanical principles and is valid in the pure as well as in the dirty limits. In pure systems the magnetoconductance oscillations are determined only by the geometrical factors. In disordered systems multiply scattered waves can reach the same point via different classically allowed diffusive paths with random phases acquired in impurity collisions; they therefore form a complicated interference picture dependent on a random potential realization in a sample. Thus, the magnetoconductance oscillations in a ring of impure metal contain a component with an amplitude and shape that reflect the features of the scatterers' distribution. This sample-specific conductance component is usually called a mesoscopic fluctuation [3–5].

The periodic conductance oscillations also contain a contribution from self-crossing paths with a closed loop circling in opposite directions, namely weak localization corrections to conductance [6–8]. It gives rise to magnetoconductance oscillations with a fundamental period of $\phi_0/2$, which are identical in macroscopically identical conductors.

It is known that magnetic scattering on spin impurities plays an important role in quantum transport [8, 9], thus the conductance of a system depends on the state of the magnetic scatterers. It was recently predicted theoretically and found experimentally that the dynamics of the subsystem of localized spins clearly manifests itself in the mesoscopic [10–15] and weak localization [15–17] effects.

In the present paper we study the influence of spin dynamics of localized spins (namely, Korringa's relaxation [18]) on the quantum conductance oscillations in a small ring of a diluted magnetic alloy where a sufficient admixture of paramagnetic impurities causes multiple magnetic scattering for the electrons contributing to current formation; thus a single electron spin relaxation length, L_s, is shorter than the length L of wires composing the ring. The following analysis is devoted both to the case of paramagnetic impurities and to the influence of their alignment in high magnetic fields. The spin-glass regime is also discussed to complete the picture.

For the formal description of the Aharonov–Bohm effect in such a system we use the Fourier representation of a conductance, $G = \langle G\rangle + \delta G$ (which contains both the mentioned regular $\langle G\rangle$ and sample-dependent δG parts), as a function of an enclosed magnetic flux ϕ. In the weak localization part of magnetoconductance oscillations, only even terms are represented,

$$\langle G_{\mathrm{WL}}\rangle = \langle G_{\mathrm{WL},0}\rangle + \sum_m \langle G_{2m}\rangle \cos(4\pi m\phi/\phi_0) \qquad (1)$$

while the mesoscopic one contains all integer harmonics,

$$\delta G_k = \delta G_0 + \sum_k \delta G_k \cos(2\pi k\phi/\phi_0 + \delta\varphi_k). \qquad (2)$$

In a 1D ring, (1) and (2) give a picture of oscillations in the whole range of magnetic fields. In realistic devices a finite magnetic flux $\delta\phi = \phi S_{\mathrm{wire}}/S_{\mathrm{ring}}$ penetrates inside the wire area. When it exceeds the flux quantum value, $\delta\phi > \phi_0$, it completely changes the interference picture of diffusive electron waves [5]. This results in random variations of amplitudes δG_k and phases $\delta\varphi_k$ from one interval to another ($\Delta H < H_c = \phi_0/S_{\mathrm{wire}}$) in a magnetic field [5]. Therefore, the mean square value, $\langle\delta G_k^2\rangle$ of the Fourier coefficients in series (2) is, in principle, a measurable quantity (as well as the ensemble averaging $\langle\ \rangle$ can be replaced by the averaging over different independent H_c intervals).

Both weak localization and mesoscopic conductance parts show sensitivity to any inelasticity in the system. The inelastic suppression of quantum effects in electronic transport was studied in detail in the weak localization [8] as well as in the mesoscopic [9] theories; in the present paper they will be left out of the discussion. That means that in the following the inelastic length is supposed to exceed the sample dimensions L. We also impose the same restriction on the temperature length [3, 19]: $L_T = \sqrt{Dh/T} \gg L$.

As to the contents of the paper, section 2 is devoted to the qualitative consideration of spin dynamics effects on mesoscopic magnetoconductance oscillations and to the definition of necessary parameters. The results of the perturbation theory calculations of $\langle\delta G_k^2\rangle$ values in the free-spin and spin-glass regimes of magnetic impurities are reported in sections 5 and 6, respectively. These calculations, as well as the model used, are described in detail in sections 3 and 4. The comparison between mesoscopic and weak localization contributions to the Aharonov–Bohm effect is presented in the appendix.

2. Effects of the spin dynamics of impurities on mesoscopic conductance fluctuations

In the following we consider a metallic ring sufficiently contaminated by magnetic impurities which interact with free electrons by the plain exchange, $V_{\rm int} = (\boldsymbol{s} \cdot \boldsymbol{S}) g \delta(x - x_{\rm imp})$. Their concentration n_s is assumed to be high enough to raise fast single electron spin relaxation by the rate $\tau_s^{-1} = g^2 S(S+1) n_s / \lambda_F^d \epsilon_F$ which provides a multiple magnetic scattering during the characteristic time $\tau_f = L^2/D$ of the electron's diffusive flight through a ring. (Here D denotes the diffusion coefficient and L is the wire length.) In this case most electron paths contain spin-flip events and, therefore, an instantaneous form of the mesoscopic part of the ring conductance depends on an instantaneous spin configuration of impurities. It has the usual mesoscopic scale e^2/h [9], but this cannot give an estimation of observable oscillations when the temporal evolution of impurity spins has to be taken into account. The latter happens because of Korringa's relaxation of localized spins due to their interaction with thermalized electrons, $\tau_K^{-1} = T g^2 / \lambda_F^{2d} \epsilon_F^2$, or with phonons. Moreover, this relaxation (with the rate $\tau_K^{-1} = eVg^2/\lambda_F^{2d}\epsilon_F^2$) exists even at zero temperature due to spin transfer from impurities to non-equilibrium current electrons.

Anyway, the spin configuration of a sample changes in time and that gives rise to random fluctuations of the instantaneous conductance value. On the other hand, an efficient temporal self-averaging of fluctuations takes place, thus reducing the mesoscopic DC effects. For example, the mesoscopic conductance fluctuations in a long wire with magnetic impurities are suppressed by the factor of $(\tau_s/\tau_f)^{3/4}$ [11] when the duration of a measurement exceeds the time scale τ_*,

$$\tau_* \approx \tau_K \tau_s / \tau_f. \tag{3}$$

(The latter was found from the condition that the reorientation probability, $(\tau_*/\tau_K)(\tau_f/\tau_s)$, of at least one of (τ_f/τ_s) impurity spins, on which an electron scatters in its diffusion through a sample along a characteristic path, is of the order of unity.) Therefore, only a small fraction of the trajectories that do not touch spin-flip events contributes to the DC-fluctuation formation. An exponentially small expectation of such a trajectory encircling a quasi-1D ring k times gives a strong suppression,

$$\delta G_k \sim \exp(-kL/L_s) \tag{4}$$

of all harmonics of mesoscopic magnetoconductance oscillations, even in systems without any inelaticity. (Here $L_s = (D\tau_s)^{1/2}$ is the spin relaxation length in a diffusive regime.)

This conclusion is valid in all the magnetic fields which are not strong enough to orientate the spins of impurities, $H\mu_{\rm imp} < T$. In the opposite case all the impurities have aligned spins. That decreases an effective spin relaxation rate, $\tau_s^{-1}(H) \approx \tau_s^{-1} e^{-H\mu_{\rm imp}/T}$ [20], and one can display the mesoscopic magnetoresistance fluctuations of the universal scale, forcing the magnetic field up to the value of $H > T/\mu_{\rm imp}$. This looks like just a transition in the amplitude of mesoscopic oscillations, as was observed experimentally in artificially contaminated mesoscopic semiconductor devices [13] and in rings of diluted magnetic alloys [14, 15].

In the case of high fields the relations between different harmonics of the Aharonov–Bohm oscillations are determined by the efficiency of electron escape from a ring to the bulk. If the contacts of a ring to the electrodes have a tunnelling character, or they are prepared in the form of short leads, then a single parameter, $\alpha = G_{\text{wire}}/G_{\text{contact}}$, can be used to describe the mesoscopic effects. When the parameter α is small, $\alpha \ll 1$, it has the meaning of a probability of an electron resting in a ring after each flight through a contact region, and the amplitude of any higher harmonics in the series (2) is suppressed by the factor α in comparison with the previous one,

$$\delta G_k \sim \alpha^k. \tag{5}$$

Consequently in the next section we study this simplified model to account analytically for the electron's escape from a ring in combination with spin-scattering effects.

3. The perturbation theory calculations

The consistent derivation of mean square values $\langle \delta G_k^2 \rangle$ of amplitudes of different harmonics of magnetoconductance oscillations is based on the calculations of the correlation function $K(\phi, \phi')$ of two DC conductances taken at different values ϕ and ϕ' of a magnetic flux. The latter can be found from the correlation function $\langle I(\phi, \eta) I(\phi', 0) \rangle$ of instantaneous current values (V is the voltage drop in a sample),

$$K(\phi, \phi') = \lim_{\theta \to \infty} V^{-2} \int_{-\theta/2}^{\theta/2} \frac{\mathrm{d}\eta}{\theta} \mathrm{d}\eta \{ \langle I(\phi, \eta) I(\phi', 0) \rangle - \langle I(\phi) \rangle \langle I(\phi') \rangle \} \tag{6}$$

and within the perturbation theory approach (the approximation of $p_F l/h \gg 1$) it is mainly determined by the diagrams shown in figure 1 [5, 21]. As to their analytical expression, it can be given in the terms of particle–hole (diffusion) and particle–particle (Cooperon) Green functions $P^{(d)}$ and $P^{(c)}$ and distribution function $N(\epsilon)$. (We can refer the reader to the reviews [8] for the rigorous definitions.)

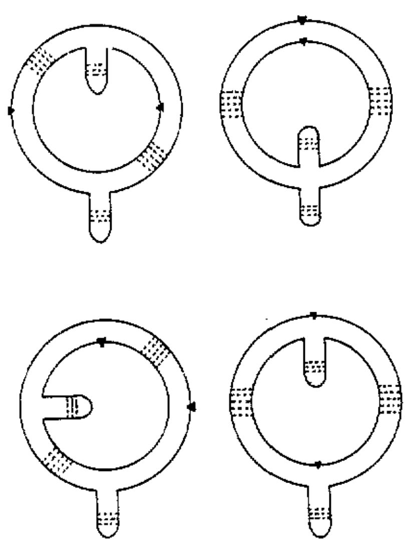

Figure 1. The main diagrams contributing to the current–current correlation function. Each of them corresponds to the infinite series summed by the means of Dyson's equation. This summation is described in detail in the reviews [8] and the expression of the current–current correlation function in terms of diffusion and Cooperons (the ladders) and the distribution function $N(\epsilon)$ (the appendices) can be found in [21].

The above-mentioned two-particle Green functions satisfy the diffusion-like equations

$$\left\{\partial_t - D\left(\nabla - \mathrm{i}\frac{e}{\hbar c}A^{(d)}\right)^2 + \frac{1}{\tau_s}(1 + d_J\mathrm{e}^{-|\eta|/\tau_K})\right\} P_J^{(d)}(t,t';\eta;x,x') = \delta(x-x')\delta'(t-t') \tag{7}$$

and

$$\left\{\partial_\eta - D\left(\nabla - \mathrm{i}\frac{e}{\hbar c}A^{(c)}\right)^2 + \frac{1}{\tau_s}(1 + c_J\mathrm{e}^{-|\eta|/\tau_K})\right\} P_J^{(c)}(\eta,\eta';t;x,x') = \delta(x-x')\delta(\eta-\eta') \tag{7'}$$

inside wires. Here a magnetic field is accounted for by the gauge term $A^{(d,c)}$, $\mathrm{rot}\,A^{(d,c)} = H \pm H'$. The coefficients c_J and d_J describe the difference of spin relaxation induced decay of singlet ($J = 0$) and triplet ($J = 1$) Cooperon and diffusion modes, respectively; $c_0 = -d_0 = 1$, $c_1 = -d_1 = -1/3$. In the limit of $\eta \to 0$ this difference gives rise to relaxation rates splitting and corresponds to the case of a frozen-spin configuration. The temporal evolution of impurity spins due to Korringa's relaxation,

$$\langle S_\alpha^{\mathrm{imp}}(0)S_\beta^{\mathrm{imp}}(\eta)\rangle = \delta_{\alpha\beta}S(S+1)\mathrm{e}^{-|\eta|/\tau_K} \tag{8}$$

is accounted for by the time-dependent factor $\exp(-|\eta|/\tau_k)$ [11]. As far as the time averaging in (6) extracts the long tail contribution to the correlation function $K(\phi,\phi')$, (7) and (7′) can be studied only in this limit in a reduced form

$$\left\{\partial_t - D\left(\nabla - \mathrm{i}\frac{e}{\hbar c}A^{(d,c)}\right)^2 + \frac{1}{\tau_s}\right\} P^{(d,c)} = \delta(x-x')\delta(t-t'). \tag{9}$$

In a mesoscopic system, (9) has to be completed with the boundary conditions at the surface and the ends of wires. The first of them have the form of flow zeroing, $\{n(\nabla - \mathrm{i}(e/\hbar c)A_{d(c)})\}P^{(d,c)} = 0$, and in a ring prepared of long and thin wires they allow us to rewrite (9) as a quasi-1D equation. After the time-variable Fourier transform it takes the form

$$\{-\mathrm{i}\omega + \tau_s^{-1} - \tau_f^{-1}(\partial_{\psi_r} - \mathrm{i}Y_r)^2 + \tau_f^{-1}(2\pi\delta\phi^{(d,c)}/\phi_0)^2\}P^{(d,c)} = \delta(\psi-\psi') \tag{10}$$

where the dimensionless variables $0 < \psi_r < 1$ denote the coordinates along two wires forming a ring ($r = 1$ means an 'up' and $r = 2$ means a 'down' semicirclet). The phases $Y_r = \pm\pi\psi_r\phi^{(d,c)}/\phi_0$ are of a gauge origin and vary from zero to $\pm\pi\phi^{(d,c)}/\phi_0$ in up and down semicirclets; $\phi^{(d)} = \phi - \phi', \phi^{(c)} = \phi + \phi'$. As was determined before, $\tau_f = L^2/D$ gives the time of a diffusive flight through a ring. Finally, the last term in the left-hand side of (10) originates from the magnetic field flux $\delta\phi$ penetrating inside the wires.

The boundary conditions at the ends of wires (at $\psi_r = 0$ and $\psi_r = 1$) can be introduced phenomenologically in the form of continuity and current conservation equations,

$$\begin{aligned} &P(\psi_1,\psi') = P(\psi_2,\psi') \\ &(\pm)\alpha^{-1}P(\psi_1;\psi') = (\partial_{\psi_1} - \mathrm{i}Y_1)P(\psi_1;\psi') + (\partial_{\psi_2} - \mathrm{i}Y_2)P(\psi_2;\psi'). \end{aligned} \tag{10'}$$

In the former the term $\alpha^{-1}P$ takes into account the electron's escape to bulk. In an open system $\alpha \to 0$ and the two semicirclets of a ring are weakly connected. An isolated ring is described by the limit of $\alpha \to \infty$. The chosen boundary conditions are rigorous for tunnelling contact of a ring with the electrodes and quite acceptable in the case of them being joined by short leads. This model provides a single-parameter description of all effects of contacts, avoiding complicated geometrical factors [22].

The meaning of a phenomenological parameter α can be clarified by the comparison of a naively suggested value of an averaged current through the system, $\langle I\rangle = V[1/2G_{\text{wire}} + 2/G_{\text{contact}}]^{-1}$, that can be calculated within the same phenomenological approach. The former,

$$\langle I\rangle = eDS_{\perp}L^{-1}\nu_{\text{f}} \int \mathrm{d}\epsilon\,[\partial_{\psi}N(\epsilon)]$$

follows from the solution of the equations representing the distribution function $N(\epsilon, \psi)$ of electrons in a ring with boundary conditions at the contacts analogous to that in (10′),

$$\begin{aligned} &\partial_{\psi}^{2}N(\epsilon,\psi) = 0 \\ &2\alpha\partial_{\psi}N = N - N_{\text{F}}(\epsilon + eV/2) \qquad \psi = 0 \\ &2\alpha\partial_{\psi}N = N_{\text{F}}(\epsilon - eV/2) - N \qquad \psi = 1. \end{aligned} \tag{11}$$

(Here $S_{\perp}$ is a cross sectional area of each wire, ν_{F} is the Fermi density of states and $N_{\text{F}}(\epsilon \pm eV/2)$ are the Fermi distribution functions in the bulk.) Thus, $\langle I\rangle = 2eVG_{\text{wire}}/(1+4\alpha)$, and it is clear that α is nothing other than the ratio of wire to contact conductances,

$$\alpha = G_{\text{wire}}/G_{\text{contact}}. \tag{12}$$

In principle, this parameter can be varied experimentally by application of different gate voltages, thus changing the contact transparency in semiconductor microdevices with joints covered by gates.

4. Low- and high-field magnetoconductance fluctuations

The solutions of (10) and (11) can be used to derive the current–current correlation function [21]

$$\begin{aligned} &\langle I(\phi,\eta)I(\phi',0)\rangle - \langle I(\phi)\rangle\langle I(\phi')\rangle \\ &\quad = \frac{3}{2}\left(\frac{e^2}{h}\right)^2 \frac{D^2}{16} \int \mathrm{d}\epsilon\,\mathrm{d}\epsilon' \int \mathrm{d}\psi\,\mathrm{d}\psi'\,\partial_{\psi}N(\epsilon)\partial_{\psi'}N(\epsilon') \\ &\qquad \times \{|P_J^{(d)}(\omega = \epsilon - \epsilon'; \psi, \psi')|^2 + |P_J^{(c)}(\omega = \epsilon - \epsilon'; \psi, \psi')|^2\}. \end{aligned} \tag{13}$$

From the above-mentioned degeneracy of the decay rates in the long-tail limit of Cooperon and diffusion one can see that their contributions to (13) are similar, thus the correlation function $K(\phi, \phi')$ can be separated into a sum of two similar additives,

$$K(\phi, \phi') = K(\phi - \phi') + K(\phi + \phi'). \tag{14}$$

Each of them can be written as

$$K(\tilde{\phi}) = \frac{3}{2}\left(\frac{e^2}{h}\right)^2 (1+4\alpha)^{-2} \sum [Q_n(\tilde{\phi})^2 + \tau_f/\tau_s + (2\pi\delta\tilde{\phi}/\phi_0)^2]^{-2} \tag{15}$$

where $Q_n(\tilde{\phi})$ are the roots of the algebraic equation

$$F(Q, \tilde{\phi}) = 2\alpha^2 Q^2[\cos 2Q - \cos(2\pi\tilde{\phi}/\phi_0)] + 2\alpha Q \sin 2Q + (1 - \cos 2Q)/2 = 0.$$

The summation of (15) results in a plain $K(\tilde{\phi})$ form

$$K(\tilde{\phi}) = \left(\frac{e^2}{h}\right)^2 \kappa \frac{1 + u\cos(2\pi\tilde{\phi}/\phi_0)}{[1 - v\cos(2\pi\tilde{\phi}/\phi_0)]^2}. \tag{16}$$

The coefficients $\kappa(\gamma, \alpha), u(\gamma, \alpha)$ and $v(\gamma, \alpha)$ depend on the decay efficiency of electron–electron and electron–hole correlation due to electron escape from a ring (parameter α), and due to the reorientation of impurity spins (parameter γ),

$$\gamma^2 = \tau_f/\tau_s + (2\pi\delta\tilde{\phi}/\phi_0)^2. \tag{17}$$

The former also describes the effect of a magnetic flux penetrating inside the wires. The limit of $\gamma \ll 1$ can be used to describe the magnetoconductance oscillations locally (within each correlation magnetic-field interval) in the regime when a high field suppresses spin-flip scattering processes. In this case only the escape to electrodes determines the amplitude and the features of the oscillation's shape, and

$$\begin{aligned} \kappa &= \tfrac{1}{15}[1 + 16\alpha + 120\alpha^2 + 384\alpha^3 + 480\alpha^4]/[(1 + 4\alpha + 2\alpha^2)(1 + 4\alpha)]^2 \\ u &= 8\alpha^2(1 + 12\alpha + 30\alpha^2)/[1 + 16\alpha + 120\alpha^2 + 384\alpha^3 + 480\alpha^4] \\ v &= 2\alpha^2/(1 + 4\alpha + 2\alpha^2). \end{aligned} \tag{18}$$

In an open system ($\alpha \ll 1$) the oscillations are weak,

$$K(\tilde{\phi}) = \frac{1}{15}\left(\frac{e^2}{h}\right)^2 \frac{1 + 8\alpha^2\cos(2\pi\tilde{\phi}/\phi_0)}{[1 - 2\alpha^2\cos(2\pi\tilde{\phi}/\phi_0)]^2}. \tag{19}$$

In a semi-closed system ($\alpha \gg 1$) they are of (e^2/h) scale and the correlation function

$$K(\tilde{\phi}) = \frac{1}{2\alpha^2}\left(\frac{e^2}{h}\right)^2 \frac{1 + 0.5\cos(2\pi\tilde{\phi}/\phi_0)}{[1 + \frac{2}{\alpha} - \cos(2\pi\tilde{\phi}/\phi_0)]^2} \tag{19'}$$

has a resonant form. It manifests itself in periodically repeated resonant conditions for the electron tunnelling between electrodes through single-particle states in the ring closed to the Fermi level. The contribution of a single resonant state to the conductance is of the order of (e^2/h). Thus one can expect that the magnetoconductance oscillations have (e^2/h) amplitude even in an almost isolated ring and look like narrow (of width $\Delta\phi \approx 2\phi_0\alpha^{-1/2}/\pi$) splashes on the background of an averaged small-ring conductance.

The conductance fluctuations in the case of a low field (when spin-flip scattering in combination with impurity spins dynamics works best) are described by the limit of $\gamma = \sqrt{\tau_f/\tau_s} \gg 1$ and the oscillations in this case are weak:

$$v = 8[\alpha\gamma e^{-\gamma}/(1+2\alpha\gamma)]^2 \ll 1$$
$$u = 2\gamma v \ll 1 \qquad \kappa = \tfrac{3}{4}(1+4\alpha)^{-2}\gamma^{-3}. \tag{20}$$

Formulae (17) and (20) can also be applied to the analysis of correlation field (H_c) behaviour. The latter can be estimated from the comparison of two additives in (17), $2\pi\delta\tilde{\phi}(H)/\phi_0 \sim \tau_f/\tau_s$; thus it is clear that the width H_c of the coherent oscillations interval gradually decreases when a magnetic field aligns the localized spins.

5. Relations between harmonics of magnetoconductance oscillations

The calculated correlation functions $K(\phi,\phi')$ can also be used for a quantitative description of experimental data. Namely, the values $\langle\delta G_k^2\rangle$ are the subject of the comparison between the above theory and those obtained in measurements, and they can be directly derived from the Fourier transforms of a single-variable function $K(\tilde{\phi})$. Thus, the mean squares of the amplitudes of mesoscopic Aharonov–Bohm conductance oscillations can be found as

$$\langle\delta G_k^2\rangle = 4\left(\frac{e^2}{h}\right)^2 \frac{\kappa}{(1-v^2)^{3/2}}\left(\frac{u+v}{v}k + (1+vu)\right)\left(\frac{1-(1-v^2)^{1/2}}{v}\right)^k \tag{21}$$

and

$$\langle\delta G_0^2\rangle = \left(\frac{e^2}{h}\right)^2 \kappa\frac{1+vu}{[1-v^2]^{3/2}}. \tag{21'}$$

In the low field region, $\mu_{\rm imp}H \ll T$, where the Zeeman splitting of magnetic states of impurities is less than the temperature, the amplitudes of all the terms in (2) are suppressed and

$$\langle\delta G_k^2\rangle = 6k\left(\frac{e^2}{h}\right)^2 (1+4\alpha)^{-2}(L_s/L)^2\left(\frac{2\alpha L/L_s}{1+2\alpha L/L_s}\exp(-L/L_s)\right)^{2k}. \tag{22}$$

In a specific mesoscopic ring the transition to the high magnetic field regime is accompanied by the transition from free to frozen aligned states of paramagnetic spins. In a magnetic field $H > (T/\mu_{\rm imp})\ln(\tau_f/\tau_s)$ the system behaves similarly to that without magnetic scattering. The only difference is that the mean square values

$$\langle\delta G_k^2\rangle = \frac{2}{3}\left(\frac{e^2}{h}\right)^2 (k+1/5)\alpha^{2k} \qquad \alpha \ll 1 \tag{23}$$

$$\langle\delta G_k^2\rangle = \frac{3}{16}\left(\frac{e^2}{h}\right)^2 \frac{(k+1)}{\alpha^{1/2}}\left(1-\frac{2}{\alpha}\right)^k \qquad \alpha \gg 1$$

are formed of independent contributions of spin-polarized electron waves, thus they give half of that in magnetically pure materials.

In addition, it is easy to extend the proposed consideration to systems with a strong spin–orbit interaction. The latter extracts the contributions of singlet modes both in the mesoscopic and weak localization cases and in the paramagnetic regime it reduces the amplitudes, $\delta G_{\mathrm{so},k}$, of mesoscopic effects by a factor of a half, $\langle\delta G^2_{\mathrm{so},k}\rangle = \langle\delta G^2_k\rangle/4$. At the same time, the weak localization terms discussed in the appendix are negligible compared with mesoscopic terms, as long as the solely surviving singlet Cooperon mode is fast decaying (an exponent in (A1) contains a shorter length $L'_s = L_s/\sqrt{2}$).

6. The Aharonov–Bohm effect in metallic spin glasses

The analogous behaviour is also specific to conductance fluctuations in the vicinity of a spin-glass transition. An extension of the calculations (6)–(13) to the case of a frozen spin field shows that the main contribution to the conductance–conductance correlation function is from the singlet diffusion mode, which is not affected by magnetic scattering in the $\tau_{\mathrm{K}} \to \infty$ limit. Thus the mean squares $\langle\delta G^2_{\mathrm{SG},k}\rangle$ in a metallic spin glass are half that in a regime of aligned spins,

$$\langle\delta G^2_{\mathrm{SG},k}\rangle = \langle\delta G^2_k\rangle/2$$

and we predict enhancement of conductance oscillations by a factor of $\sqrt{2}$ close to the magnetic field destroying the frozen disordered spin state.

Besides that, the correlation function $K(\phi,\phi')$ contains information about the phases of oscillations. The separable form (14) of $K(\phi,\phi')$ represents the cosine-like oscillations inside the first H_c interval in the paramagnetic limit (in good agreement with the Onsager rules applied to the conductance problem in a non-magnetic 1D system). On the other hand, in the spin-glass regime the suppression of the second ($(\phi+\phi')$-dependent) term manifests an arbitrary phase of the low-field Aharonov–Bohm effect, even in the 1D case. This statement does not contradict the Onsager relations: a frozen spin configuration violates time reversibility independently of a magnetic field and opens the way to the linear magnetoconductance dependence [23, 24].

The above-mentioned Cooperon suppression in metallic spin glasses immediately gives the suppression of weak localization corrections to conductance. Thus the spin-glass materials present the exclusive case when the Aharonov–Bohm effect is purely mesoscopic in the whole range of magnetic fields.

7. Conclusions

To summarize, in the present paper it is shown that the Aharonov–Bohm oscillations of the DC-conductance of a mesoscopic ring of a magnetic alloy are strongly suppressed because of the dynamical evolution of the spin configuration of scatterers. An alignment of paramagnetic spins by a magnetic field, $H \gg T/\mu_{\mathrm{imp}}$, forbids spin-flip processes and displays magnetoconductance oscillations with an amplitude determined by ring contacts with electrodes. Thus the low- to high-field transition in a paramagnetic system is followed by the transition in the amplitude of magnetoconductance oscillations. One can expect an analogous enhancement of oscillations in spin-glass materials close to the magnetic field which destroys the frozen disordered magnetic phase. The reported theory gives the quantitative analytical description of the Aharonov–Bohm effect in a quasi-1D ring using the minimal number of device parameters.

Acknowledgments

I thank Professor D E Khmel'nitskii for useful advice, Professor A D Stone for information and A Benoit for detailed discussions of the results in reference [14] prior to their publication. I also thank O Fal'ko for her help in the work on the text. I am grateful to Professor P Wyder for hospitality and to the German–Isralien Foundation for Science Research & Development, grant no G-112-279.7/88, for support during this research.

Appendix. Weak localization contribution to the Aharonov–Bohm effect

Finally, we compare the mesoscopic contribution to the Aharonov–Bohm effect with the weak localization contribution calculated in the framework of the model (7′)–(10′). In these calculations the conventional relation between quantum correction to conductance (the sum of the diagrams shown in figure 2) and the Cooperon [7, 8] was *exploited*,

$$\langle G_{\mathrm{WL}}\rangle = V^{-1}\frac{eD}{2\pi h L}\int \mathrm{d}x \int \mathrm{d}\eta \int \mathrm{d}\epsilon\, \nabla N(\epsilon, x) \times \left[P_0^{(c)}(\eta, -\eta, \epsilon, x, x) - 3P_1^{(c)}(\eta, -\eta, \epsilon, x, x)\right]$$

and, as it follows from (6′), there exist two regimes of weak localization in magnetic alloys depending on Korringa's relaxation intensity [17]. One of them occurs at the lowest temperatures where Korringa's time τ_{K} is much longer than the time τ_{f} of diffusion along a characteristic path, which is responsible for the weak localization contribution to the Aharonov–Bohm effect. In this case the relaxation of localized spins is not sufficient and the decay rates of singlet and triplet Cooperon modes in (7′) are split ($1/\tau_{\mathrm{s},0}^{(c)} = 2\tau_{\mathrm{s}}^{-1}$ and $1/\tau_{\mathrm{s},1}^{(c)} = 2\tau_{\mathrm{s}}^{-1}/3$). Thus the long living triplet mode dominates the quantum corrections to conductivity [8] and at the lowest temperatures only the weak localization terms (1)

$$\langle G_{2k}\rangle = -\frac{3}{\pi}\frac{e^2}{h}\frac{1}{1+4\alpha}\frac{L_{\mathrm{s}}'}{L}\left(\frac{2\alpha L/L_{\mathrm{s}}'}{1+2\alpha L/L_{\mathrm{s}}'}\exp(-L/L_{\mathrm{s}}')\right)^{2k} \tag{A1}$$

determine even harmonics of oscillations. Here $L_{\mathrm{s}}' = \sqrt{3/2}L_{\mathrm{s}}$ is the decay length of a triplet mode. At higher temperatures an opposite inequality between τ_{K} and τ_{f} returns us to the case of degenerate decay rates ($\tau_{\mathrm{s},j}^{-1} = \tau_{\mathrm{s}}^{-1}$) of both Cooperon modes [17]; in this case the advantage of weak localization over mesoscopic terms results from the temperature smearing of mesoscopic effects due to cancellation of

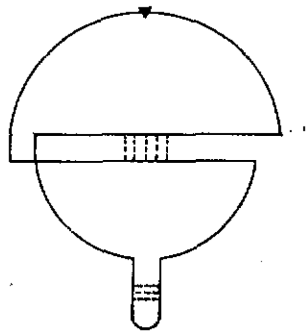

Figure 2. The diagrams which correspond to weak localization corrections to conductance.

random contributions from uncorrelated spectral intervals [19]. All in all, we conclude that in the mesoscopic system with allowed spin-flip scattering, all even harmonics of the Aharonov–Bohm effect are of weak localization origin.

To compare, in systems with no magnetic scattering the amplitudes of the weak localization contribution to magnetoconductance oscillations,

$$\langle G_{2k}\rangle = -\frac{4e^2}{3\pi h}\alpha^{2k} \qquad \alpha \ll 1 \tag{A2}$$

$$\langle G_{2k}\rangle = -\frac{e^2}{\pi h}\alpha^{-1/2}\left(1-\frac{2}{\alpha}\right)^k \qquad \alpha \gg 1$$

are numerically (when $\alpha \ll 1$) or even parametrically (when $\alpha \gg 1$) smaller than those of mesoscopic origin. They are also negligible in the spin-glass regime, as follows from the corresponding Cooperon suppression [16].

References

[1] Aharonov Y and Bohm D 1959 *Phys. Rev.* **115** 485

[2] Gefen Y, Imri Y and Azbel M Ya 1984 *Phys. Rev. Lett.* **52** 129
Buttiker M, Imri Y and Azbel M Ya 1984 *Phys. Rev.* A **30** 1982

[3] Altshuler B L 1985 *JETP Lett.* **41** 648
Lee P A and Stone A D 1985 *Phys. Rev. Lett.* **55** 1622

[4] Webb R A, Washburn S, Umbach C P and Laibowitz R B 1985 *Phys. Rev. Lett.* **54** 2696

[5] Stone A D 1985 *Phys. Rev. Lett.* **54** 2692
Altshuler B L and Khmel'nitskii D E 1985 *JETP Lett.* **42** 359

[6] Sharvin D Yu and Sharvin Yu V 1981 *JETP Lett.* **34** 272

[7] Altshuler B L, Aronov A G and Spivak B Z 1982 *JETP Lett.* **33** 94

[8] Lee P A and Ramakrishnan T V 1987 *Rev. Mod. Phys.* **57** 287
Altshuler B L, Aronov A G, Khmel'nitskii D E and Larkin A I 1982 *Quantum Theory of Solids* ed I M Lifshitz (Moscow: MIR) p 130

[9] Lee P A, Stone A D and Fukuyama H 1987 *Phys. Rev.* B **35** 11039
Stone A D 1989 *Phys. Rev.* B **39** 10736

[10] Altshuler B L and Spivak B Z 1986 *JETP Lett.* **42** 447
Feng Sh, Bray A J, Lee P A and Moore M A 1987 *Phys. Rev.* B **36** 5624

[11] Bobkov A A, Fal'ko V I and Khmel'nitskii D E 1990 *Sov. Phys.–JETP* **71** 393
Fal'ko V I 1990 *Proc. 20th Int. Conf. on the Physics of Semiconductors (Thessaloniki, 1990)* ed E M Anastassakis and J D Joannopoulos (Singapore: World Scientific) p 2319

[12] Chandrasekhar V, Santhanam P and Prober D E 1990 *Phys. Rev.* B **42** 6823

[13] Hiem A, Dubonos S and Antonova I 1990 *JETP Lett.* **52** 873

[14] Benoit A 1990 private communication
[15] de Vegvar P G N, Levy L P and Fulton T A 1991 *Phys. Rev. Lett.* **66** 2380
[16] Wei W, Bergmann G and Peters R-P 1988 *Phys. Rev.* B **38** 11751
[17] Fal'ko V I 1991 *JETP Lett.* **53** 340; 1991 *Sov. Phys. Low Temp.* **17** 1173
[18] Korringa J 1959 *Physica* **16** 601
[19] Stone A D and Imry Y 1986 *Phys. Rev. Lett.* **56** 189
[20] Amaral V S 1990 *J. Phys.: Condens. Matter* **2** 8201
[21] Fal'ko V I and Khmel'nitskii D E 1989 *Sov. Phys. JETP* **68** 186
Khmel'nitskii D E and Larkin A I 1986 *Phys. Scr.* T **14** 4
[22] Serota R A, Feng Sh, Kane C and Lee P A 1987 *Phys. Rev.* B **35** 5031
Kane C, Lee P A and DiVincenzo D P 1988 *Phys. Rev.* B **38** 2995
DiVincenzo D P and Kane C 1988 *Phys. Rev.* B **38** 3006
Santhanam P 1989 *Phys. Rev.* B **39** 2541
[23] Buttiker M 1988 *IBM J. Res. Dev.* **32** 317
[24] Hershfield S 1991 *Phys. Rev.* B **44** 3320